

FAR-IR AND MM PROPERTIES OF QUASARS

P. Andreani¹, A. Franceschini¹ G.L. Granato²

¹Dipartimento di Astronomia di Padova, vicolo dell'Osservatorio 5, I-35142 Padova, Italy.
e-mail: andreani/franceschini@astrpd.pd.astro.it.

² Osservatorio Astronomico, vicolo dell'Osservatorio 5, I-35142 Padova, Italy.
e-mail: granato@astrpd.pd.astro.it.

ABSTRACT

We use photometric data, from the optical to the *mm*, for a large sample of optically selected radio-quiet quasars, at low and high redshifts, to test emission models from circum-nuclear dusty torii around them. Model parameters, such as dust mass, temperature distributions and torus sizes are inferred, under the assumption that the dust is heated only by the central nuclear source. Dependences of best-fit parameters on luminosity and redshift are studied and the contribution of dust in the host galaxy to the observed fluxes is briefly mentioned. Only tentative conclusions can be drawn from this yet large dataset and detailed modelling, because crucial spectral information is missing at wavelengths where the QSO dust emission is more prominent, i.e. at $\lambda \simeq 50$ to $600 \mu\text{m}$. Poor information in this wavelength range affects our understanding not only of the high-redshift objects, but also of the low-redshift sample. We then expect fundamental contributions by the FIRST mission in this field, which is obviously related to the more general one of galaxy formation.

Keywords: AGNs, dust emission, dust mass evolution

1. INTRODUCTION

While disk galaxies appear to form their stellar content at moderate rates during most of the Hubble time, there are no clear indications yet that the expected bright phase of star formation in spheroidal galaxies has been detected by optical searches. A possible explanation is that galaxies in this phase are shrouded in dust, produced in large amounts by the early generations of massive stars (e.g. Franceschini et al. 1994; De Zotti et al. 1996).

This idea of an early and quick metal and dust production affecting optical emission at least in bulge-dominated massive galaxies may receive some support by preliminary evaluations of the dust content in high-*z* quasars and of (very high) metal abundances in absorption line systems "associated" to the QSO.

These have shown that the close environments of high-*z* (both radio-loud and radio-quiet) QSOs were the site of quick and efficient star formation and metal production (Haehnelt & Rees 1993; Franceschini and Gratton 1997). Indeed, the presence of an AGN could even mask the presence of a forming spheroid and complicate its investigation, but can also be exploited to identify target areas where to look for forming structures (galaxies, galaxy clusters and groups).

Sub-*mm* - *mm* observations are then starting to shed light into these phases. The chance of detection of high-*z* objects at these wavelengths is favoured by the strong and positive K-correction implied by the steeply rising sub-*mm* spectra.

Many high-*z* sources, most of which associated with active nuclei, have been recently detected in the millimeter (both in the continuum and CO line emission; see Andreani et al. 1993; Chini and Krügel 1994; Dunlop et al., 1994; Isaak et al. 1994; McMahan et al., 1994; Ivison 1995; Ohta et al., 1996; Omont et al., 1996a and 1996b). With the exclusion of radio-loud quasars, such radiation has been attributed to dust since the observed spectrum, $F \propto \nu^{3-4}$, is far too steep for any dominant synchrotron self-absorbed contribution.

In this contribution we make use of a large sample of optically selected quasars at low and high redshifts, observed in the far-IR to *mm* region, to study dust emission in radio-quiet objects and its possible dependence on redshift. The basic assumption in this analysis is that the dust distribution, assumed to have simple axial symmetry, either confined to the quasar nucleus or covering a sizeable fraction of the hosting galaxy, is illuminated by the central nuclear source. Obvious evidence in support of this is the dominance of the point-like nuclear source in the optical in both high- and low-redshift objects.

This effort marks a significant improvement over previous studies, as it exploits the whole spectral information from the optical to the *mm*, the optical providing in particular an essential datum on the intensity of the radiation field illuminating the dust.

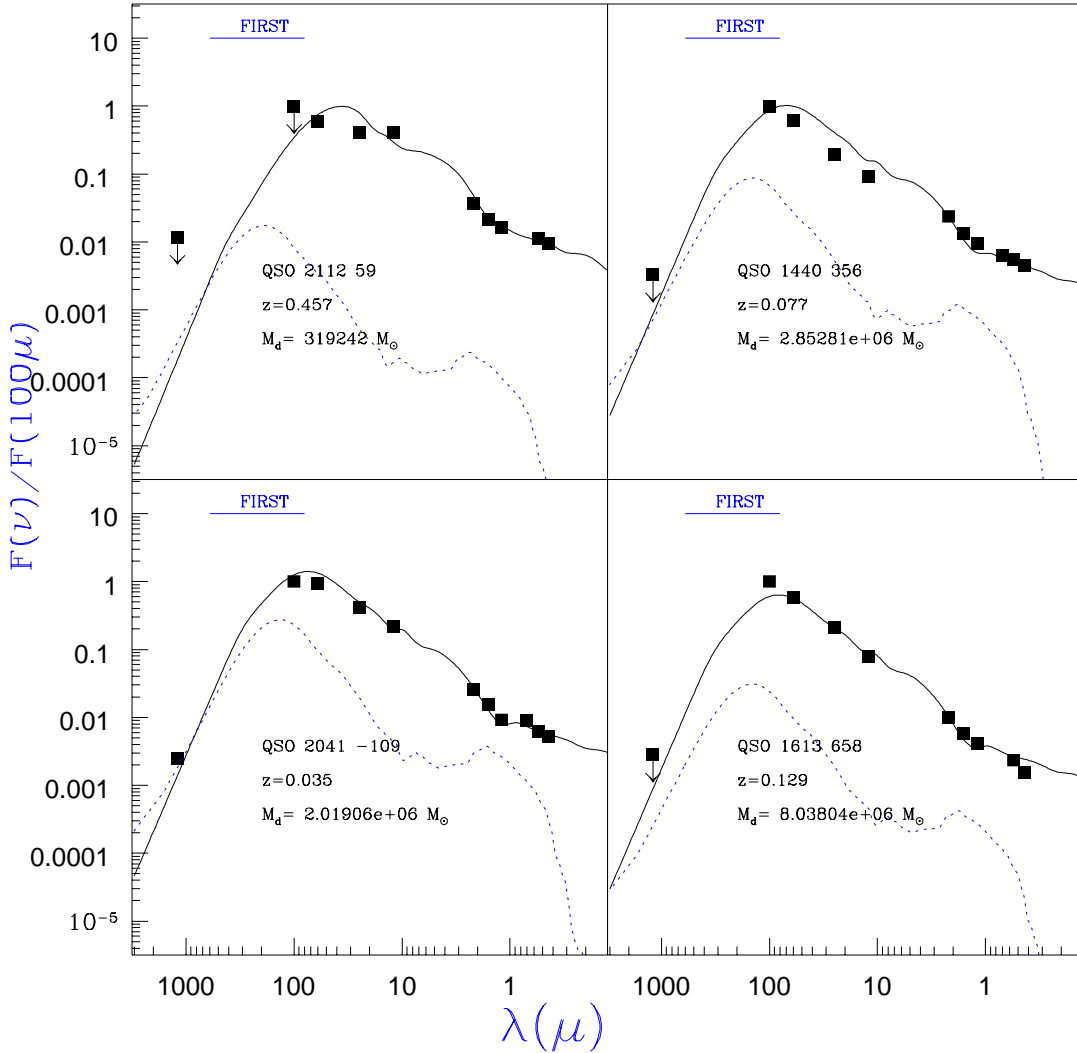


Figure 1. Observed SEDs of low- z AGNs fitted with the model described in §3 (solid line) with the parameters $\frac{r_{max}}{r_{in}}$, Θ , A_V : (a) 200, 0° , 18 (b) 1000, 0° , 40 (c) 1500, 0° , 40 (d) 1500, 0° , 40. Dotted-line curve corresponds to the spectrum of a typical spiral galaxy with a dust mass of $\sim 10^7 M_\odot$

2. THE SAMPLE

The sample consists of optically selected quasars with sub- mm and mm observations. Far-IR data are from the IRAS PSC, and for most of the sources co-added survey data were provided by IPAC based on the SCANPI procedure. Mm observations are partly collected from the literature and partly taken by the authors with the IRAM 30m at Pico Veleta. The low-redshift sample consists mainly of PG radio-quiet quasars.

3. MODELS OF DUST EMISSION IN QUASARS

The model spectral energy distributions (SEDs) used to fit the observational data were computed with the numerical code described by Granato & Danese (1994), which solves the radiative transfer equation in a circumnuclear dust distribution. This step is required since in the torii predicted by unified models the dust emission is self-absorbed in the near- and mid-IR. The code is quite flexible about the geometry and composition of the dusty medium, the only restriction being axial symmetry, and thus allows a wide exploration of the parameter space.

We assume in our exploration that the optical properties of dust are the same for all sources, with a standard Galactic composition. The inner radius r_{in} of the dust distribution is set by the grain sub-

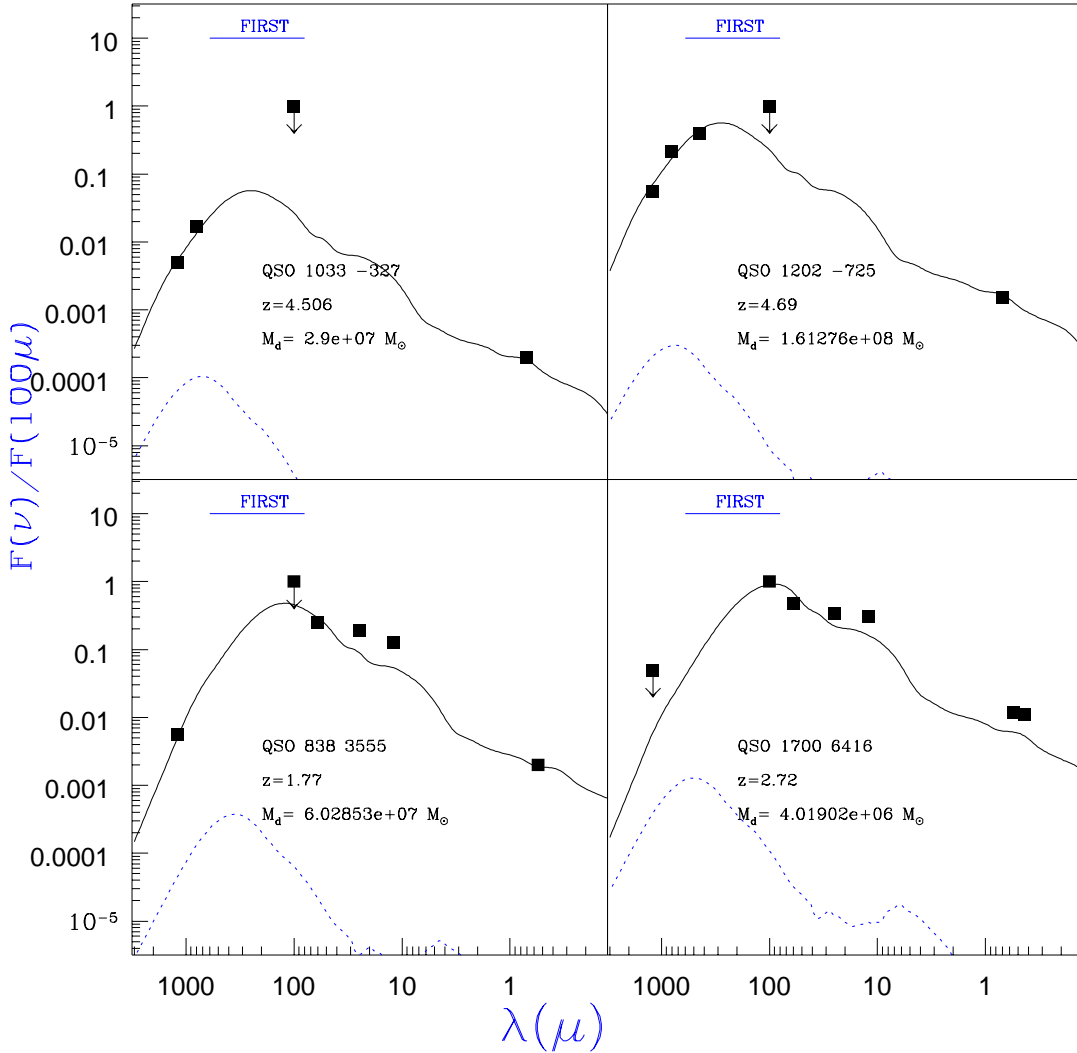


Figure 2. As figure 1 but for high- z AGNs (a) 600, 0° , 40 (b) 800, 0° , 40 (c) 600, 0° , 30 (d) 200, 0° , 18

limation condition, at $T_s = 1500$ for graphite and $T_s = 1000$ for silicates. This translates into the condition $r_{in} \sim 0.5\sqrt{L_{46}}$ pc, where L_{46} is the luminosity of the primary optical–UV emission in units of 10^{46} erg s^{-1} .

The details of the model, as well as the effect of the various free parameters, have been widely discussed by Granato & Danese 1994 and in Granato, Danese & Franceschini (1997). Here we focus on the simplest geometry which is in reasonable agreement with the available observations, the “flared disc”, in which the scale height of the torus along the z -axis increases linearly with the radial distance, and the dust distribution within the disc is homogeneous. Model parameters are then (i) the outer radius r_{max} of the dust distribution; (ii) the absorption A_V along typical obscured directions; and (iii) the covering factor $f = \cos(\Theta_h)$ of the torus, where Θ_h is the half opening angle of the dust-free cones. In practice, the free parameters in the fit were the former two, the last one having been fixed to $f = 0.8$, a value not incon-

sistent with requirements of unified models of AGNs (Granato et al. 1997).

Roughly speaking, the first parameter is related to the broadness of the IR bump arising from dust reprocessing, whilst the second controls mainly the near-IR slope of the SEDs as observed from obscured directions as well as its anisotropy. Therefore A_V is in principle constrained by the SEDs of obscured AGNs or by testing the anisotropy of mid-IR emission. The covering factor is obviously related to the relative power reprocessed by the dust in the IR bump and the primary optical continuum flux.

In this simple geometry the total dust mass is given by the product between the disc volume $V = \frac{4}{3}\pi \cos \Theta_h$ and the constant dust density $\rho = \frac{\tau_\nu}{k_\nu(r_{max}-r_{in})}$, where k_ν is the absorption coefficient per unit dust mass and τ_ν the equatorial optical thickness. This gives:

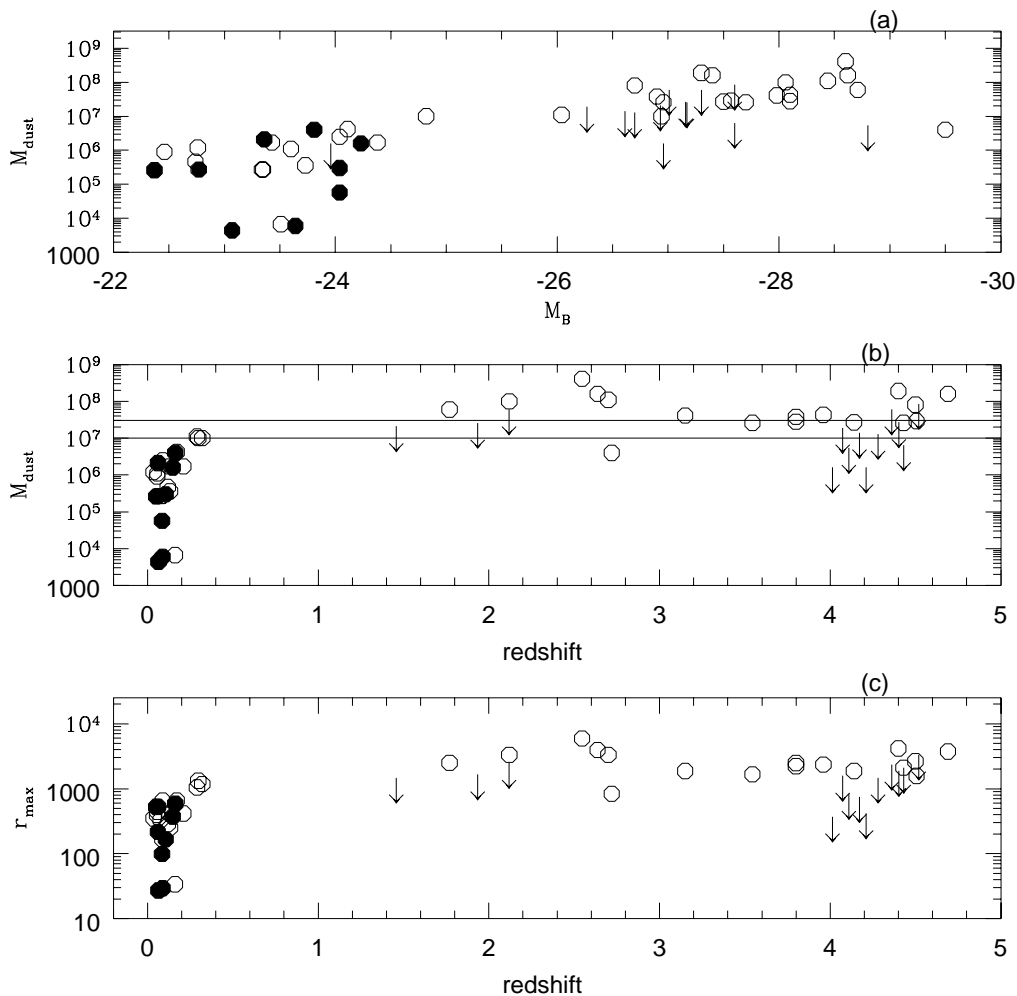


Figure 3. Dust masses versus (a) B-band absolute magnitude and (b) redshift. (c) Maximum size of the dust emission region as a function of redshift. Filled circles correspond to objects for which the presence of a host galaxy is required to improve the fit at $\lambda > 60\mu\text{m}$. Horizontal lines in (b) show the range of dust masses found in nearby spirals.

$$\frac{M_{\text{dust}}}{M_{\odot}} \sim 0.2 \left(\frac{r_{\text{max}}}{r_{\text{in}}}\right)^2 \left(\frac{L}{L_{46}}\right)^{3/2} \cos \Theta_h A_V \quad (1)$$

Unless otherwise stated, all quantities are computed assuming $H_0=50$ km/s/Mpc and a flat universe ($q_0 = 0.5$).

4. RESULTS

Figures 1 and 2 show typical spectra of 4 low- z and 4 high- z sources. Some information on the source and model parameters are reported in the figure panels and captions. The thick solid curves are the best fits SEDs, while the dotted line is the broad-band optical- mm spectrum of a typical spiral galaxy, used

for comparison. Clearly, while for local objects the hosting galaxy can contribute to some extent at the longest wavelengths, for high- z quasars the observed spectra are far in excess of what would be expected from a redshifted SED of a normal galaxy. This reflects in part the much increased power of the illuminating source, following the well-known evolution with z of the primary continuum.

The overall quality of the fits is remarkably good, if we consider that only two parameters (r_{max} and A_V) are free to model the spectral shape.

Figure 3a plots the best-fit dust mass, M_d , as a function of the B-band absolute magnitude, M_B , showing the expected trend of increasing M_d at increasing M_B . A similar trend is observed with the AGN bolometric luminosity.

Figure 3b shows the evolution of the AGN M_d versus redshift. The filled circles correspond to those objects for which the contribution of the host galaxy is important.

Figure 3c plots the best-fit outer radius r_{out} of the

dust distribution versus redshift. M_d and r_{out} are very tightly related in our model, both being precisely constrained by the long wavelength (mm or sub- mm) flux data. Therefore, the plots in Figs. 3b and 3c display quite a similar behaviour.

In both cases the low- z objects show widely dispersed values in the parameters, with typically moderate values for the dust mass, $M_d \sim 10^5 - 10^7 M_\odot$ and from 10 pc to 1 kpc for r_{max} . For the high- z subsample, typical values for M_d and r_{max} are larger, with M_d typically in excess of 10^7 and r_{max} in excess of 1 kpc.

Note that the procedure of the dust mass estimation is quite a robust one: we believe that uncertainties in the model parameters affect its value by less than a factor two, and the basic conclusions are not affected.

5. DISCUSSION

Some limitations of the present analysis have to be considered before drawing any conclusions.

The first is that the observational SEDs are interpreted assuming that most of the IR- mm flux comes from dust illuminated by the AGN itself and that the dust in the flared disc is homogeneously distributed from the inner sublimation surface up to kpc-scale distances.

For most of the local objects only upper limits to the mm fluxes are available. So, it cannot be excluded that for some of these we are missing significant contributions of cold dust from the hosting galaxy at $\lambda \geq 100\mu m$ (most of the mm observations were collected with large antennas fed with single channel bolometers, having therefore a field of view limited to a few arcsec). Indeed, Danese et al. (1992) and Rowan-Robinson (1995) already suggested that the FIR spectrum at $\lambda \geq 60\mu m$ in low-luminosity AGN may be contributed by cold dust in the surrounding galaxy situated at large radial distances from the AGN and with typical dust masses of 1 to $3 \cdot 10^7 M_\odot$.

The relative contribution at far-infrared wavelengths of the nuclear and extended component will only be settled by high resolution mapping with planned large mm arrays (e.g. LSA).

On the other hand, the SEDs of high- z object SEDs are less constrained, as only a few spectral data are available for each source, due to the fact that IRAS was not sensitive enough to detect a significant number of them (a couple of exceptions appear in Fig. 2). In these cases the sub- mm data are the only information we have on the circum-nuclear interstellar medium, IRAS providing a weak constraint on the dust temperature distribution. Comparison of our model to the data suggests the existence of a large gaseous structure around the nucleus (with 1-5 kpc radius), including a dust mass of up to a few $10^8 M_\odot$, and a corresponding gas masses of typically 10^{10} to $10^{11} M_\odot$.

We note, in particular, the large values of the outer radius of the dust distribution, which are dictated by

the combined constraints set by the mm flux, the primary optical field intensity and the IRAS upper limits. Such extended distributions indicate that they are not merely circum-nuclear dust torii, as seen in local Seyfert galaxies, but have rather scale-lengths comparable with those of the bulge of the putative host galaxy.

In principle, we would expect that our estimate of the dust mass M_d in quasars and the size r_{max} of the dust distribution should be unaffected by the power of the primary continuum and by its evolution with cosmic time. In practice an obvious bias operates in Figure 3: the more luminous AGNs found at the higher z are also likely to be hosted by higher mass galaxies. Small mass objects at high- z escape detection and the lower right part of the plot cannot be sampled by present instruments.

What is clear is that no high mass objects are found in the nearby universe.

A way to explain the trends observed in Figs. 3b and 3c would be to assume that we are sampling the same class of objects. Evolution in the dust mass content in quasars could then be related to the history of galaxy evolution, as revealed by optical deep surveys: a *downsizing* process is taking place, such that more massive galaxies form at higher redshift, followed by a sequence of less and less massive objects forming at lower and lower redshift down to the formation of dwarfs.

However, this opens the question of the fate of the dust: where has all this dust gone? Was it swept away from the quasar? Was it consumed to form stars in a late phase of star formation? Note that the difference between low and high redshift objects would be further enhanced in an open universe: dust masses at redshifts larger than 2 for $\Omega \sim 0.01$ are higher by a factor between 2 and 5.

The alternative possibility is that we are observing at high- and low-redshifts two distinct populations. Environmental conditions at high redshifts could favour the formation of higher mass black holes, while low- z AGNs may be related to the refueling of small dead black holes in late type galaxies, where gas is still available (Haehnelt & Rees 1993).

Because of a selection bias (all sources were optically selected), no edge-on objects were found in the present sample: the nuclear source is not totally obscured from the circumnuclear torus. Obscured sources, of which IRAS F10214 could represent the prototype, can only be found from FIR/sub- mm surveys such as those expected with the FIRST Satellite.

An abundant population of dusty objects could heretofore escape detection. Are many early quasars obscured by the products of massive galaxy-forming starbursts? Such objects might observationally appear very much like ultraluminous infrared galaxies, so that sub- mm photometric surveys by FIRST represent the only way to discover them.

ACKNOWLEDGEMENTS

We would like to thank L. Danese and S. Cristiani for instructive discussions. Part of the data used in this work were taken with the SCANPI procedure, developed by the NASA Archival center for IRAS Satellite (IPAC) operating by JPL.

REFERENCES

- Andreani P., La Franca F, Cristiani S., 1993, MNRAS 261, L35
- Chini R., Kreysa E., Biermann P.L., 1989a, A&A, 219, 87-97
- Chini R., Biermann P.L., Kreysa E., Gemünd H.P., 1989b, A&A, 221, L3-L6
- Chini R., and Krügel E., 1994, A&A 288, L33
- Danese L. et al. 1992, ApJ 399, 38
- De Zotti G. et al. 1996, in *Science with Large Millimetre Arrays*, Ed. P. Shaver, ESO, Springer Verlag
- Dunlop J.S., Hughes D.H., 1994 Nat 370, 347
- Franceschini A. et al. 1994, ApJ 427, 140
- Franceschini A, Gratton R., 1997 MNRAS 286, 235
- Granato G.L., Danese L., 1994 MNRAS 268, 235
- Granato G.L., Danese L., Franceschini A., 1997 MNRAS in press
- Haehnelt M.G., Rees M.J. 1993, MNRAS 263, 168
- Isaak K.G., McMahon R.G., Ellis R.E., Withington S., 1994, MNRAS 269, L28
- Iverson R.J. 1995, MNRAS 275, L33
- McLeod K.K., Rieke G.H. 1995, ApJ 454, L77
- McMahon R.G. et al. 1994, MNRAS 267, L9
- Ohta K. et al. 1996, Nature 382, 426
- Omont A. et al. 1996a, Nature 382, 428
- Omont A. et al. 1996b, A&A 315, 1
- Rowan-Robinson, M., 1995 MNRAS 272, 737
- Sawicki M.J., Lin H., Yee H.K.C. 1997 AJ 113, 1
- Wickramasinghe N.C. et al 1995, MNRAS 276, L9